 doi:10.20944/preprints202104.0047.v2

Article

Synthesis and evaluation of AlgNa-g-poly(QCL-co-HEMA) hydrogels for cartilage tissue engineering and controlled release of betamethasone.

Jomarien García-Couce [1,2], Marioly Vernhes [3], Nancy Bada [2], Lissette Agüero [2], Oscar Valdés [4], José Alvarez-Barreto [5], Gastón Fuentes [1,2,*], Amisel Almirall [1,2] and Luis J. Cruz [1]

[1] Centro de Biomateriales, Universidad de La Habana, La Habana, Cuba; jgcouce@gmail.com (J.G-C.); bada@biomat.uh.cu (N.B.); lissetteaguerol@gmail.com (L.A.); amisel.almirall@gmail.com (A.A.)
[2] TNI Group, Department of Radiology, Leiden University Medical Center (LUMC), Leiden, The Netherland; L.J.Cruz_Ricondo@lumc.nl
[3] Laboratorio de Biología Molecular. Departamento de Radiobiologia. Centro de Aplicaciones Tecnológicas y Desarrollo Nuclear (CEADEN), mariolys@ceaden.edu.cu
[4] Centro de Investigación de Estudios Avanzados del Maule (CIEAM), Vicerrectoría de Investigación y Posgrado, Universidad Católica del Maule, Talca, Chile; ovaldes@ucm.cl
[5] Department of Chemical Engineering. Universidad de San Francisco de Quito. Ecuador; jalvarezb@usfq.edu.ec

* Correspondence: gastonfe@gmail.com or gastonfe@biomat.uh.cu

Abstract: Hydrogels obtained from the combination of different polymers are an interesting strategy for the development of controlled release system platforms and tissue engineering scaffolds. In this study, the applicability of sodium alginate-g-(QCL-co-HEMA) hydrogels for these biomedical applications was evaluated. Hydrogels were synthesized by free-radical polymerization using different concentration of the components. The hydrogels were characterized by Fourier transform infrared spectroscopy, scanning electron microscopy, and swelling degree; betamethasone release as well as the *in vitro* cytocompatibility with chondrocytes and fibroblast cells were also evaluated. Scanning electron microscopy confirmed the porous surface morphology of the hydrogels in all cases. The swelling percent was determined at different pH and was observed to be pH-sensitive. The controlled release behavior of betamethasone from the matrices was investigated in PBS media (pH = 7.4) and the drug was released in a controlled manner up to 8 h. Human chondrocytes and fibroblasts were cultured on the hydrogels. The MTS assay shown that almost all hydrogels are cytocompatibles and an increase the proliferation in both cell types after one week of incubation was observed by Live/Dead® assay. These results demonstrate that these hydrogels are attractive materials for pharmaceutical and biomedical applications due to their characteristics, their release kinetics and biocompatibility.

Keywords: Hydrogels; Sodium alginate; Betamethasone; Drug delivery; Cartilage tissue engineering

1. Introduction

Articular cartilage is a highly specific, avascular, connective tissue that lines the end of each bone that forms the joint, providing a smooth and gliding surface. It is predominantly formed of water, proteoglycans and type II collagen and chondrocytes are the only cells that composes it [1, 2]. Osteoarthritis (OA) is the most common affection suffered by cartilage, a disease characterized by the loss of the matrix and its functionality producing inflammation and severe pain, which are usually treated with anti-inflammatory drugs. Corticosteroids (eg. dexamethasone, triamcinolone, betamethasone) are frequently used in the treatment of OA due to their potent anti-inflammatory activity and it has been proved that low dose exerts effects on down-regulating the gene expression level of MMPs

 doi:10.20944/preprints202104.0047.v2

(MMP-1, MMP-3, and MMP-13) in chondrocytes, reducing glycosaminoglycans loss [1]. However, their prolonged administration causes many side effects. In more advanced stages of the disease and due to the limited capacity for self-repair, replacement or induced regeneration of damaged area is often required [3]. To date, different treatment methods have been designed, such as mosaicplasty, osteochondral allograft transplantation, and autologous chondrocyte implantation, among others. However, there are still limitations to produce cartilage with full biological activity [2, 4], so tissue engineering continues to be an interesting and promising alternative to repair cartilage defects in a functional way and apply more localized treatments to reduce side effects [5, 6].

Hydrogels are three-dimensional polymeric structures, capable of retaining large amounts of water or fluids without dissolving or losing their integrity. Due to these characteristics, they have a high similarity to living tissues, and they are suitable platforms for tissue engineering, drug-carrying matrices, artificial articular cartilage, and smart devices to external stimuli such as pH and temperature [7]. The use of natural polymers such as polysaccharides for developing of these matrices has been frequently studied for past decades. Chitosan, hyaluronic acid, and sodium alginate are among the most widely used [3]. Sodium alginate is a linear anionic polysaccharide, composed by B-D mannuronic acid and a-L-guluronic acid units, obtained mainly from brown marine algae [8, 9]. Due to its properties (biocompatible, biodegradable and non-toxic) several materials have been developed from alginate such as microparticles, hydrogels and films for applications in biomedical field [10]. Specifically, sodium alginate hydrogels have a similar structure to natural extracellular matrix, and for that reason their use in tissue engineering and drug delivery has grown exponentially [10, 11]. Previous studies in the field of cartilage tissue engineering have shown that its application does not produce synovitis or degenerative cartilage changes, promote adhesion and proliferation of chondrocytes to increase the deposition of glycosaminoglycans and aggrecans in the matrix, increasing the articular cartilage restoration [9]. However, hydrogels obtained only from natural polymers are mechanically weak due to the large amount of water they absorb. As a solution to this limitation, synthetic polymers are usually added to improve the physicochemical properties of hydrogels. Among the synthetic polymers poly(2-hydroxyethyl methacrylate) (HEMA), a neutral hydrophilic polymer, has been one of most used in tissue engineering due to its versatile properties such as biocompatibility, good mechanical properties, and ease of synthesis [4, 5, 12]. Hydrogels for cartilage tissue engineering from the combination of polymers, natural (eg chitosan, collagen) and synthetic (polyethylene glycol and polyvinyl alcohol) have been reported by several authors [4, 10, 13]. 2-acryloyloxyethyl trimethyl ammonium chloride (QCL) is a positive charged monomer composed by a polymerizable double bond and a quaternary ammonium at the end of its structure. According to previous reports, compounds with quaternary ammonium groups in their structure have been used as vectors to target therapeutic agents (anti-inflammatory and osteoarthritis modifying drugs) towards the cartilage, and to interact with sulfate and carboxyl groups present in the proteoglycans of ECM [14-17]. It is known that QCL's homo- and copolymers are highly charged structures, capable to interact through electrostatic attractions with other opposite charge compounds [15, 17-19]. Their inclusion in hydrogels designed for cartilage tissue engineering provides an additional benefit because they improve the tissue- material interaction.

In this work, AlgNa-g-poly(QCL-co-HEMA) hydrogels were prepared by radical copolymerization of HEMA and QCL in the presence of AlgNa and N,N-methylene diacrylamide (MBA) as crosslinking agent. Although there are some similar reports on systems based on these components, this specific composition has not been reported, or studied as a drug carrier and platform for chondrocytes incorporation. The structure and morphology were analyzed by Fourier transform infrared spectroscopy (FTIR) and scanning electron microscopy (SEM). The swelling capacity was measured as a function of time and pH. The betamethasone release from the prepared matrices in phosphate buffered saline (PBS) was evaluated. Furthermore, its cytocompatibility *in vitro* with C-28 and 3T3 cells

Preprints (www.preprints.org) | NOT PEER-REVIEWED | Posted: 6 April 2021 doi:10.20944/preprints202104.0047.v2

using MTS and live/dead assays was evaluated. All analyzes were carried out based on the composition of the hydrogels.

2. Results and Discussion

2.1. AlgNa-g-poly(QCL-co-HEMA) hydrogels

The hydrogels were obtained by a mechanism of copolymerization and simultaneous chemical crosslinking as is shown in Figure 1. Initially, the thermal decomposition of the potassium persulfate (KPS, initiator) occurs, generating the anionic sulfate radicals. Next the radicals interact with -OH group of AlgNa, extracting the hydrogen to form the corresponding macroradicals. These macroradicals act as active centers through which the grafting of QCL and HEMA monomer molecules in the main chains of AlgNa begins, chains propagation and simultaneous cross-linking process with MBA occur forming the three-dimensional graft copolymer AlgNa-g-poly(QCL-co-HEMA). Mechanisms similar to this proposed were reported in previous works and in other systems [20-23]

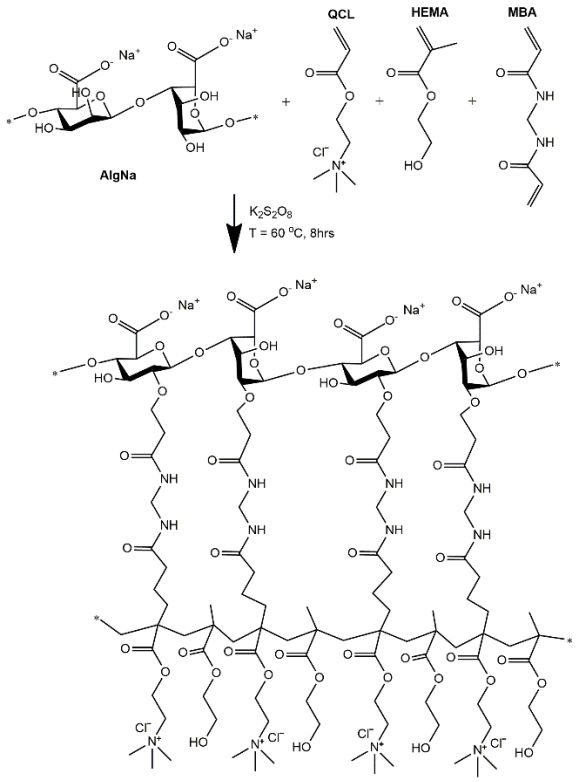

Figure 1. Schematic representation of chemical structures of polymer, monomers, and possible cross-linked structure of AlgNa-g-poly(QCL-co-HEMA) hydrogels.

2.2. Hydrogel characterizations

2.2.1. FTIR spectroscopy analysis

FT-IR spectroscopy was used to confirm the structure of the hydrogels prepared, the spectrums of initial pure components and some samples of hydrogels are shown in Figure 2. Figure 2a shows the spectrum of AlgNa, the broad band at 3258 cm^{-1} cans be attributed to -OH stretching vibration. Others characteristics signals observed at 1598 and 1403 cm^{-1} are attributed to asymmetric and symmetric stretching vibration bands of $-COO^-$ group [22]. Signals at 1080, 1025 and 813 cm^{-1} correspond to stretching vibrations of asymmetric and symmetric -C-O-C, and Na-O respectively [24]. Both monomers employed have C = O and C = C groups in their structure whose characteristic peaks are observed at 1718 and 1636 cm^{-1} in the QCL spectra (figure 2b) [25, 26] and at 1711 and 1636 cm^{-1} in case of HEMA (figure 2c) [27, 28]. In the QCL spectrum, other characteristic peaks are also observed at 1478 and 1185 cm^{-1} attributed to the bending band of quaternary ammonium groups ($-N^+(CH_3)_3$) and C-O of ester, respectively [25, 29]. In 950 cm^{-1} appears a singular

Preprints (www.preprints.org) | NOT PEER-REVIEWED | Posted: 6 April 2021 doi:10.20944/preprints202104.0047.v2

band related to the C–N stretching of quaternary ammonium groups [30]. In addition to the C=O and C=C characteristic bands, HEMA shows intense signals at 940 and 813 cm^{-1} associated to -C=C- group [31], at 1160 and 1076 cm^{-1} corresponding to C-O-C stretching vibrations of ester group [21, 28]. In the hydrogel spectrums (figure 2d, 2e, 2f) all absorption bands mentioned above are presents, some of them, overlapped. The signals between 1720 and 1724 cm^{-1} are due to C=O stretching frequency, while those between 1070 and 1185 cm^{-1} are caused by the stretching frequencies of C-O-C bonds of ester groups, demonstrating the presence of the QCL and HEMA units in the gel network. Additionally, the intensity of bands at 1478 and 950 cm^{-1}, ascribed to QCL, increases between the spectrum 2d and 2f due to the increase of QCL in the hydrogel's composition. Signals at 1598 cm^{-1} are due to the C=O of the carboxylate group of alginate, whereas, band at 1025 cm^{-1} is owing to the symmetric C-O-C stretching frequencies. In addition, asymmetric stretching vibration of COO^{-} group of alginate at 1402 cm^{-1} remains almost the same in the hydrogels indicating not chemical interactions occurs during the hydrogel's obtention process [23]. On the other hand, the bands at 1636, 940 and 813 cm^{-1} associated to the C=C stretching vibration were not found in the spectrum of the samples H2 and H4 (figure 2d, 2e), while the spectrum 2f shows a little band at 1636 cm^{-1}. This result was only observed for sample H6, which contains the highest percent of QCL which is a charged monomer and also has three methyl linked at the end of the chain forming a bulky group. Both conditions can cause the approach between the monomer units to be limited, which implies that their inclusion in the growing polymer chains is reduced and therefore some unreacted monomer remained, causing the corresponding signal of methylene.

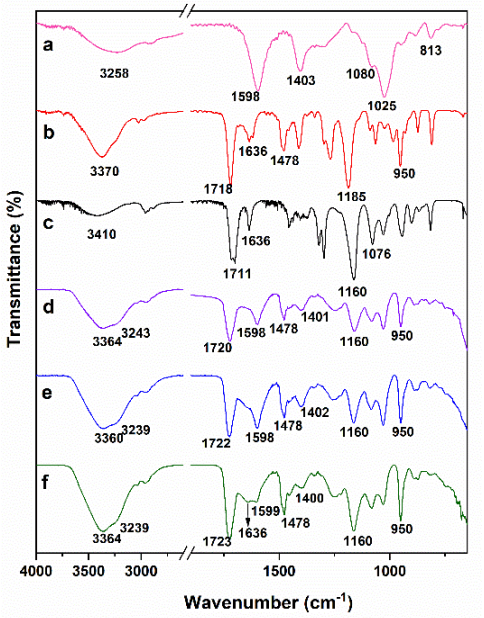

Figure 2. FTIR spectra of AlgNa (a), QCL (b), HEMA (c), hydrogel H2 (d), hydrogel H4 (e), hydrogel H6 (f)

2.2.2. Morphology characterization

The Figures 3a-3f show the SEM micrographs of the internal morphology of AlgNa-g-poly (QCL-co-HEMA) hydrogels. It is observed that all the samples have a porous structure and the pore size, although it varies, does not show a marked difference respect to variation of the sample's composition. In the SEM images can also be defined that hydrogels have interconnected pores through which the water molecules or fluids can easily spread and, therefore, act on the swelling degree and rate of the material, as well as constitute as sites of interaction of external stimuli such as pH or temperature. This porous structure is appropriated to allow attachment, growth, and proliferation of cells inside the matrix.

Preprints (www.preprints.org) | NOT PEER-REVIEWED | Posted: 6 April 2021 doi:10.20944/preprints202104.0047.v2

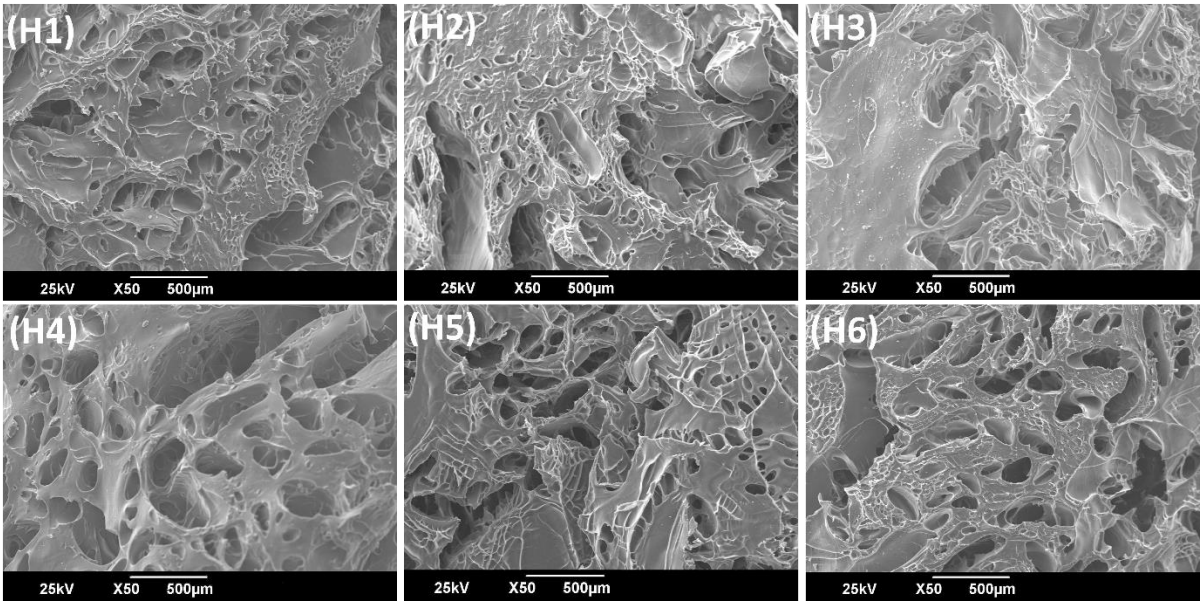

Figure 3. Scanning electron microscopy images of AlgNa-g-poly (QCL-co-HEMA) hydrogels

2.2.3. Swelling studies

The swelling process of hydrogels is conditioned by different factors, within the matrix composition and pH of the medium have been extensively studied. The matrices developed in this research are composed by three components, each one of them contributes with a functional group with hydrophilic characteristics (-COOH, $-N^{+}(CH_3)_3$, $-OH^{-}$). Now, these groups can in turn undergo interactions with each other depending on the pH of the medium, for which the swelling process in the hydrogels under study will be strongly influenced by their composition and the pH of the medium. Figures 4a and 4b show the swelling profiles of the hydrogels at pH 2.0 and 7.4 respectively, and Figure 4c shows the maximum swelling at equilibrium in more detail.

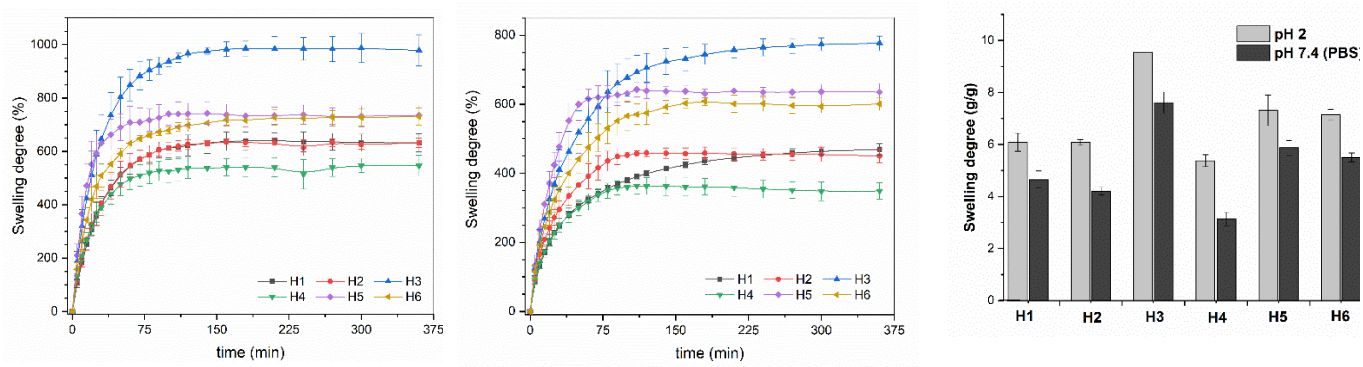

(**a**) (**b**) (c)

Figure 4. Swelling studies. (a) and (b) hydrogels' profiles at pH 2.0 and 7.4 respectively, and (c) maximum swelling at equilibrium in more detail.

The results show there is a significant difference in the swelling of the hydrogel samples at different pH. It can be seen that the swelling degree is higher at pH 2.0 than at pH 7.4 in all compositions, contrary to what is described in the literature for matrices containing AlgNa in their structure [32, 33]. This result is due to the AlgNa has a pKa between 3.2-4.0, so at pH 7.4 the carboxylic groups of its units are in carboxylates form ($-COO^{-}$) and can be linked through electrostatic interactions with the $N^{+}(CH_3)_3$ groups of QCL (Figure 5) causing a shrink of the chains and the matrix to become more compact, reducing

Preprints (www.preprints.org) | NOT PEER-REVIEWED | Posted: 6 April 2021 doi:10.20944/preprints202104.0047.v2

the fluid rate entry. At pH 2.0 the carboxylate ions are protonated and the carboxyl group is in acid form, hence electrostatic interactions do not occur. In addition, can be observed that at pH 7.4 the swelling degree of the hydrogel change depending on the composition, samples containing 20% AlgNa in their composition have less swelling compared with samples to have 10%, which reaffirms that electrostatic interactions caused by AlgNa structure have a major role in the swelling process.

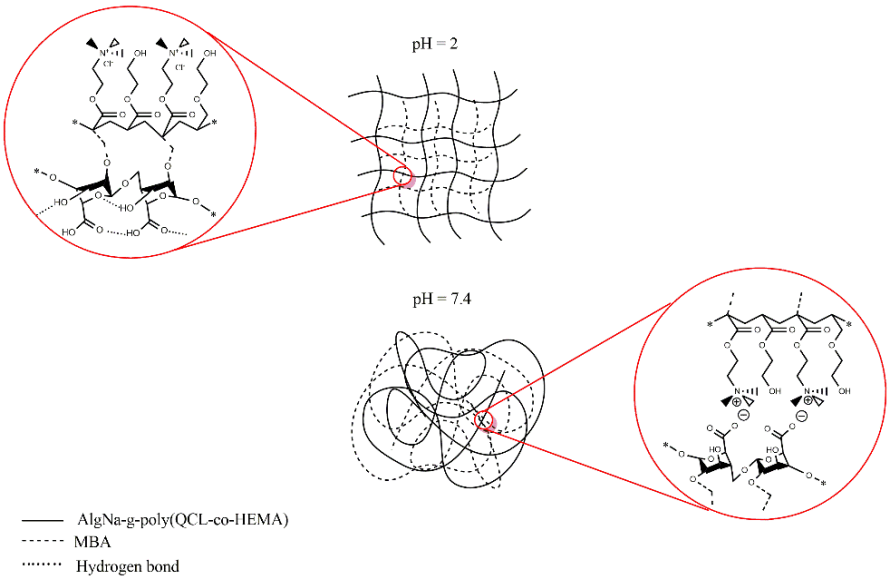

Figure 5. Schematic representation of the interactions between of functional groups in the polymeric network chains at pH 2.0 and pH 7.4

It is also valid to discuss the fact that at pH 2.0, despite electrostatic interactions do not occur, hydrogels show a similar swelling behavior to the one observed at pH 7.4 regarding to the composition of the materials. In this case, hydrogen bond formation between carboxylic groups with each other and with OH^- groups of the sugar moiety of the AlgNa structure, are the predominant interactions produced, which act as a barrier that strengthen the polymeric network and hinder the entrance of water molecules inside the hydrogel network [32, 34]. For this reason, at pH 2.0 samples with 20% alginate also have less swelling compared to 10% AlgNa samples.

2.2.3.1. Kinetic swelling study

To have a more detailed idea of how the swelling process matrix takes place, the experimental data were analyzed using Equation (2). The results are shown in Table 1. It can be seen that the value of n for all samples, both in swelling at pH 2 and PBS, is between 0.5 and 1; therefore, it can be deduce that the swelling occur by an anomalous process according to the model proposed. That is, in the swelling process the diffusion phenomenon is simultaneously accompanied by the viscoelastic relaxation of the polymer chains (both processes have similar rates). In a previous work published by Goel et al. [12], in which the influence of the inclusion of a cationic monomer on the swelling process of hydrogels of 2-hydroxyethylmethacrylate-co-[2-(methacryloyloxy)ethyl] trimethyl ammonium chloride was evaluated, values of n greater than 0.5 were reported even with the addition of small quantities of the cationic monomer, and when increased, n values also increases reaching values close to 1. According to the research conclusions, this occurs because the charged segments present in the hydrogel will repel each other to open the matrix and cause a more rapid diffusion of the water into the interior. In our work, this approach is not totally valid because the matrix contains AlgNa, which is an anionic polysaccharide whose $-COO^-$ groups, as mentioned above, will be linked by electrostatic interactions with the $N^+(CH3)_3$ groups of the QCL causing a contraction of the polymeric

Preprints (www.preprints.org) | NOT PEER-REVIEWED | Posted: 6 April 2021 doi:10.20944/preprints202104.0047.v2

network that reduces the rate of diffusion of the surrounding fluid into the matrix. Therefore, relationship between the concentration of QCL and the value of n will not be as proportional as can be seen in the results obtained by Goel *et al*.

Table 1. Swelling kinetic constant (k), transport exponent (n) and coefficient of determination (R^2) according to Equation 2

Samples	pH = 2.0			PBS, pH = 7.4		
	k	n	R^2	k	n	R^2
H1	38 ± 3	0.55 ± 0.02	99.67	33 ± 2	0.74 ± 0.02	99.90
H2	40 ± 4	0.60 ± 0.03	99.56	41 ± 3	0.69 ± 0.03	99.79
H3	52 ± 4	0.60 ± 0.03	99.55	65 ± 3	0.69 ± 0.02	99.93
H4	35 ± 1	0.59 ± 0.01	99.97	47 ± 2	0.64 ± 0.01	99.95
H5	45 ± 4	0.71 ± 0.03	99.80	68 ± 6	0.72 ± 0.03	99.84
H6	49 ± 3	0.59 ± 0.02	99.72	53 ± 2	0.69 ± 0.02	99.95

2.3. Betamethasone release study

2.3.1. FTIR characterization of BTM loaded hydrogels

To identify the BTM in the hydrogels once charged, as well as to identify possible interactions between the matrix and the drug, a study was carried out using FTIR spectroscopy of the empty and loaded hydrogels. In Figure 6 are shown the FTIR spectrums of pure BTM, three samples of AlgNa-g-poly(QCL-co-HEMA) hydrogels empty and loaded with BTM. In the FTIR spectra of pure BTM (Figure 6g) the characteristic absorption bands of this compound can be observed.

The signals observed at 1717 and 1658 cm^{-1} correspond to the C=O stretching vibration in carbonyl group of the chain and the ketonic group of ring # 1 in the cortisol structure [35, 36]. Additionally, bands at 1173 and 1086 cm^{-1} are attributed to asymmetric and symmetric stretching vibration of -C-O. The signals seen at 981 and 888 cm^{-1} can be attributed to P–O stretching vibration in phosphate moiety, and C–C skeleton vibration in cyclopentane ring, respectively [36, 37].

In the spectra of the loaded hydrogels, the characteristic bands of the BTM present in the spectrum of pure BTM are observed. As can be seen, there are no significant changes in the peaks, which evidences that there is no demonstrable chemical interaction between the hydrogel networks and the groups present in the drug molecule. The drug is then trapped in the matrix only by physical interactions.

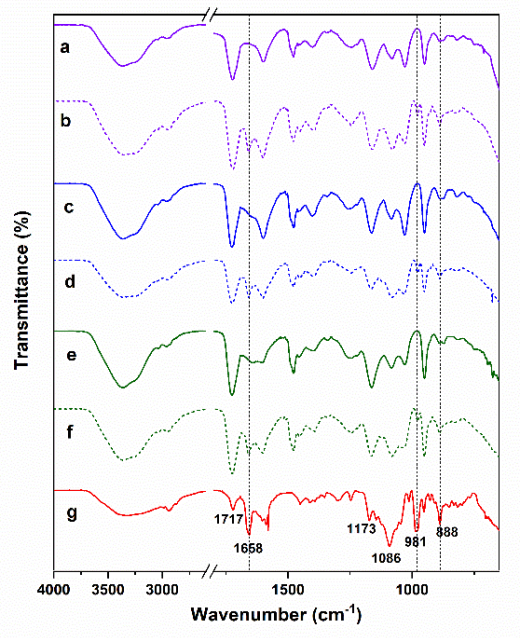

Preprints (www.preprints.org) | NOT PEER-REVIEWED | Posted: 6 April 2021 doi:10.20944/preprints202104.0047.v2

Figure 6. FTIR spectra of BTM (g), hydrogel H2 empty and loaded (a and b), hydrogel H4 empty and loaded (c and d), hydrogel H6 empty and loaded (e and f)

2.3.2. Drug release study

After immersion of the betamethasone-loaded hydrogels in a PBS solution, the amount of BTM released gradually increased over time as can be seen in Figure 7. For none of the samples a burst is observed, which evidences that the drug it is homogeneously distributed in the matrix and is not accumulated only on the material surface. The release study was carried out for 8 hours, it was observed that the samples H6 and H4 release all the encapsulated content before the fifth hour of study, the sample H5 release reaches almost 100% during the studied time, while the rest of the samples (H2, H3 and H1) released 95, 91 and 83% respectively.

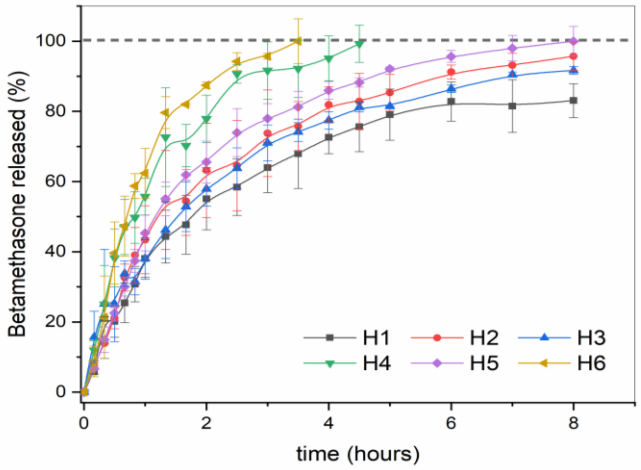

Figure 7. Cumulative *in vitro* release study of Betamethasone from AlgNa-g-poly(QCL-co-HEMA) hydrogels in PBS, pH = 7.4

The release processes are influenced by different factors such as solubility of the encapsulated drug, crosslinking and material composition, external factors such as pH or temperature and possible interactions between encapsulated drug and components of the polymeric matrix. According to the observed results, it can be deduced that in our case the swelling degree is not the fundamental variable that affects the drug release process since there is no direct relationship between the swelling degree previously determined and the release rate obtained for each sample. On the other hand, and taking into account that the encapsulated BTM is a phosphate sodium salt, so it is totally soluble in PBS, we can also rule out this factor as a variable determining the behavior of the release process. Then, evaluating the composition of the material we can observe (as summarized in Table 2) that when the concentration of HEMA in the matrix increases, the release of BTM decreases and additionally; for the same concentration of HEMA when the concentration of AlgNa increases the drug release decreases as well. Considering the describe behavior and the molecular structure of BTM in which there are acceptor sites capable of forming hydrogen bonds (H-bond acceptor) such as the oxygens of the phosphate group located at the end of the molecule [38, 39], it can be deduced that a strong interaction between the drug molecules and OH groups present in HEMA and AlgNa is taking place, whereby the increase of these in the matrix reduces the drug released.

Table 2. Relation between hydrogels composition and amount of BTM released

Samples	Composition (%)			BTM released (%)
	HEMA	QCL	AlgNa	
H6	10	80	10	100*
H4	10	70	20	100**

Preprints (www.preprints.org) | NOT PEER-REVIEWED | Posted: 6 April 2021 doi:10.20944/preprints202104.0047.v2

H5	20	70	10	99.7
H2	20	60	20	95.5
H3	30	60	10	91.4
H1	30	50	20	83.2

*BTM released before 4 h
**BTM released before 5 h

2.3.3. Kinetic drug release study

In order to know the kinetic mechanism of encapsulated BTM release, the *in vitro* experimental data were adjusted to the equation of Korsmeyer-Peppas kinetic model, which is very useful when more than one mechanism is involved in the drug release or when accurate mechanisms are unknown [40]. As can be seen in Table 3, all the calculated n values are above 0.5 and the correlation coefficient with this model was high ($R^2 > 0.96$). For samples H1 to H5, the value of n is between 0.5 - 1, indicating that the BTM released follows a non-Fickian diffusion mechanism, in which the drug released by diffusion and relaxation of the polymer chains occurs simultaneously. However, in the sample H6 the value of n is slightly higher than 1, which implies that the release is controlled by a Case II diffusion, where the diffusion of the drug towards outside of the matrix occurs very quickly compared to the chain relaxation processes, which explains the accelerated release suffered by the drug in this matrix.

Table 3. Drug release rate constant (k), diffusion exponent (n) and coefficient of determination (R^2) according to Korsmeyer-Peppas model

Samples	Korsmeyer-Peppas		
	k	n	R^2
H1	2.7 ± 0.6	0.63 ± 0.05	97.53%
H2	1.8 ± 0.6	0.76 ± 0.08	96.24%
H3	4.4 ± 0.7	0.54 ± 0.04	98.28%
H4	2.9 ± 0.9	0.73 ± 0.08	97.82%
H5	1.0 ± 0.1	0.93 ± 0.04	99.55%
H6	1.0 ± 0.4	1.0 ± 0.1	98.57%

2.4. Cytocompatibility studies

For the practical application of hydrogels in different biomedical fields, one of the most important property is that the developed material does not have inherent cytotoxicity. *In vitro* cytotoxicity standard ISO 10993-5 states that "reduction of cell viability by more than 30% is considered a cytotoxic effect". In this study, the cytotoxicity of the blank hydrogels was investigated in C-28 and 3T3 cells and the results of MTS assay are presented in Figures 8a and 8b respectively.

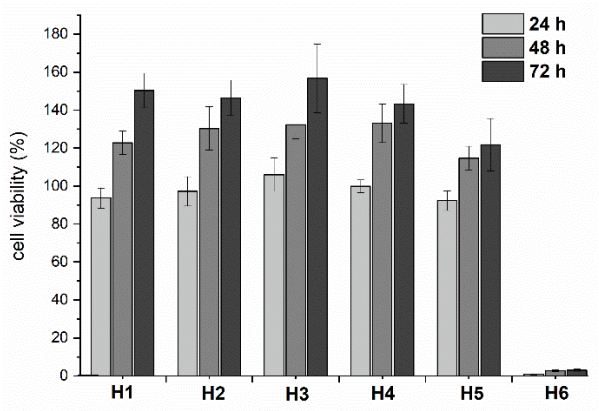

(a)

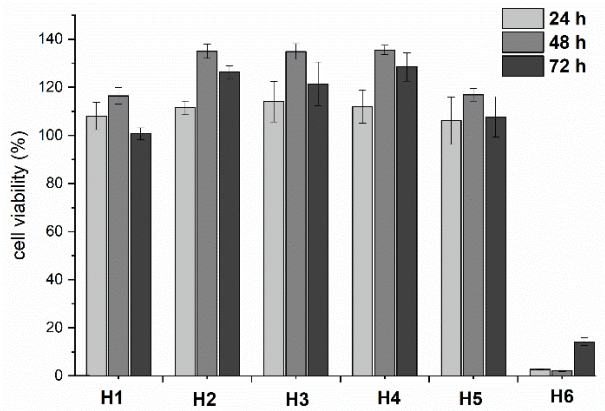

(b)

Preprints (www.preprints.org) | NOT PEER-REVIEWED | Posted: 6 April 2021 doi:10.20944/preprints202104.0047.v2

Figure 8. Cytotoxicity evaluation of the hydrogels extracts exposed to C28 (a) and 3T3 (b) cells using MTS assay method

The results show that the viability of the hydrogel extract-treated cells was higher than 90% after 24 h and even higher than 100% after 48 and 72 h of study in samples H1 to H5. The cell viability values obtained indicate that these materials are non-cytotoxic and also favor proliferation against the cells studied. Conversely, sample H6 shows high cytotoxicity for both cells evaluated, the number of viable cells being less than 20% in both kind of cell culture when they interact with the hydrogel extract in all evaluated time. This could be conditioned by the previous result obtained in the FTIR analysis, where the signal corresponding to vinylic group is observed indicating that unreacted monomer is present in the hydrogel and it is knowing monomers are molecules with a high toxicity.

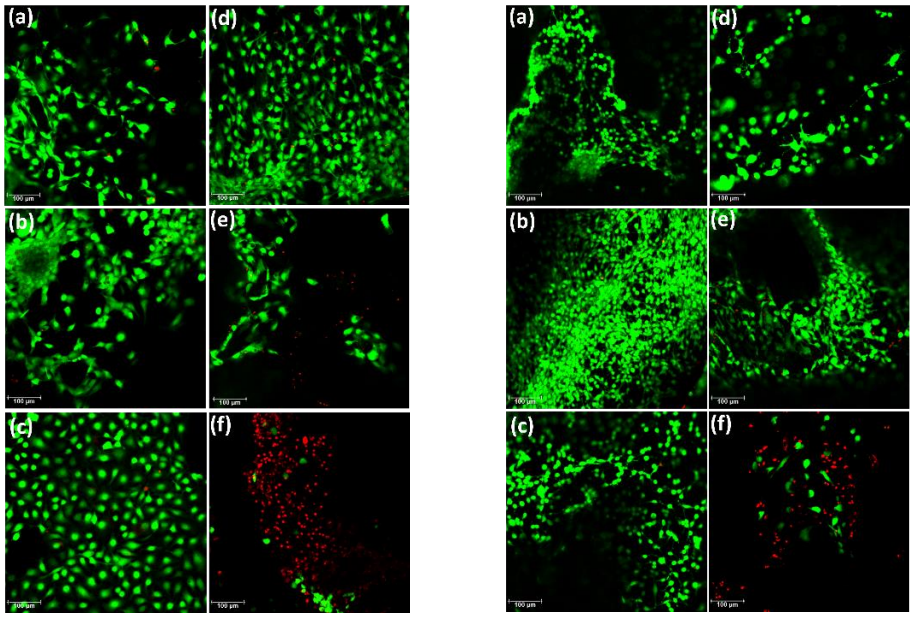

(a) **(b)**

Figure 9. A) Microphotographs of C28 cells seeded on AlgNa-g-poly(QCL-co-HEMA) hydrogels after 7 days, a)H1, b)H2, c)H3, d)H4, e)H5, f)H6. **B)** Microphotographs of 3T3 cells seeded on AlgNa-g-poly(QCL-co-HEMA) hydrogels after 7 days, a)H1, b)H2, c)H3, d)H4, e)H5, f)H6.

After quantitative analysis results obtained by MTS assay a qualitative analysis was carried out via the LIVE/DEAD assay to visualize the distribution of living and dead cells after 7 days seeded in different samples of AlgNa-g-poly(QCL-co-HEMA) hydrogels. Figures 9A and 9B show the microphotographs of cells seeded on each hydrogel after the staining. In the microphotographs obtained for the samples from H1 to H5 (Figure 9A(a,b,c,d,e) and 9B(a,b,c,d,e) most cell observed are alive. Additionally, it can see that cells are spread on the hydrogel's surfaces and elongated morphologies are also observed which is sign that cells are healthy. In some images is possible observe cells grouped forming colonies which also shows that the environment where they seeded is favorable for their proliferation. On the contrary, in the sample H6 the number of cells dead are higher than alive cells, which is in agreement with the result obtained by the MTS assay discussed above.

According to the set of results obtained, it can concluded that the AlgNa-g-poly(QCL-co-HEMA) hydrogels, samples from H1 to H5, are biocompatibles against C28 and 3T3 cells, demonstrating their potentiality as a scaffold for cartilage tissue engineering and drug delivery system

3. Materials and Methods

3.1 Materials

Preprints (www.preprints.org) | NOT PEER-REVIEWED | Posted: 6 April 2021 doi:10.20944/preprints202104.0047.v2

Commercial 2-hydroxyethylmethacrylate (HEMA, Sigma-Aldrich), 2-acryloxyethyl-trimethylammonium chloride (QCL, AQUATECH), potassium persulfate (K2S2O8, Fluka), N, N methylenebisacrylamide (MBA, Merk). Sodium alginate from Macrocystis periferia was purchased from Sigma Chemical Co. (Germany). Dulbecco's phosphate buffered saline (PBS), Dulbecco's modified eagles medium (DMEM, high glucose, with glutamaxTM), fetal bovine serum (FBS), penicillin, streptomycin, were purchased from Life Technologies (Breda, The Netherlands). 3-(4,5-dimethylthiazol-2-yl)-5-(3-carboxymethoxyphenyl)-2-(4-sulfophenyl)-2H-tetrazolium (MTS, Promega), Calcein-AM/ethidium homodimer-1 LIVE/DEAD assay kit (Invitrogen).

3.2. Preparation of AlgNa-g-poly(QCL-co-HEMA) hydrogels

AlgNa-g-poly(QCL-co-HEMA) hydrogels were prepared by graft copolymerization of QCL and HEMA onto the sodium alginate (AlgNa) chain in the presence of potassium persulfate (, 1% w/w) as thermal initiator and N, N methylenebisacrylamide (MBA, 2% w/w) as a crosslinking agent. The composition of the hydrogels is listed in Table 4, the final volume of the mixture used was 10 mL. Briefly, the calculated amount of AlgNa was dissolved in 5 mL of distilled water, then the monomer mass determined for each formulation, KPS and MBA were added under constant stirring. The final solution was placed in a glass tube, degassed for 30 min in a N_2 atmosphere to eliminate the dissolved oxygen in the system and sealed under vacuum. The glass tubes were placed in a thermostatic water bath at 60°C for 12 h. The hydrogels obtained were cut into discs for later studies.

Table 4. Composition in reaction mix of different hydrogels (total mass 2 g)

Sample	QCL (%)	HEMA (%)	AlgNa (%)
H1	50	30	20
H2	60	20	20
H3	60	30	10
H4	70	10	20
H5	70	20	10
H6	80	10	10

3.3. Hydrogel characterizations

3.3.1. Instrumental analysis

Dried hydrogel samples were characterized by Fourier transform infrared (FT-IR) spectroscopy and scanning electron microscopy (SEM). The FT-IR spectra were obtained on a Shimadzu IRSpirit-T spectrophotometer (Japan), equipped with an attenuated total reflectance accessory (ATR). The absorption spectra were recorded in the spectral range from 4000–600 cm^{-1} with a resolution of 4 cm^{-1} for 32 scans. Scanning electron microscopic observations were performed to visualize pores and morphology of the hydrogels using a SEM-JEOL JSM-6360LV microscope (Japan). Small pieces of hydrogels were sectioned and freeze-dried to observe the internal structure. The samples were placed on an aluminum mount, sputtered with gold palladium, and then scanned at an accelerating voltage of 25 kV

4.3.2. Swelling studies

The swelling kinetics of the terpolymeric hydrogels were studied in different medias (HCl, pH 2.0 and PBS, pH 7.4). The samples previously weighed were immersed in 20 mL of each swelling medium at 37°C in a thermostatic bath for 24h to reach the swelling equilibrium. At stablish time intervals the hydrogels were carefully taken out from the solution, the excess of water on the surface was removed with a filter paper, and then were weighted. In all the experiments, the water uptake was determined by gravimetric measurements using an analytical balance. The swelling degree was calculated as follows:

$$swelling\ degree\ (\%) = \frac{w_s - w_d}{w_d} \times 100 \qquad (1)$$

Preprints (www.preprints.org) | NOT PEER-REVIEWED | Posted: 6 April 2021 doi:10.20944/preprints202104.0047.v2

Where w_s and w_d are the weights of the swollen and dry hydrogels respectively. Experiments were carried out by triplicate.

In order to determine the mechanism of diffusion of the pH 2.0 solution and PBS into the hydrogels, the following equation was.

$$\frac{w_t}{w_\infty} = Kt^n \qquad (2)$$

Where K is a kinetic constant characteristic of the polymer system, w_t is the mass of solvent absorbed at time t, w_∞ is the mass of solvent absorbed at equilibrium and n is an empirical number called as transport exponent. Equation 2 is applied to the initial stages of swelling up to 60%. A value of n = 0.5 is taken as an indication that the process is diffusion controlled (Fickian diffusion) or Case I transport, whereas for n = 1.0 the swelling is considered to be controlled by the chains relaxation (Case II transport) ,and when the value of n lies between 0.5 and 1.0 the process is considered as anomalous (non-Fickian diffusion which is a combination of diffusion and relaxation) [12].

3.4. Betamethasone in vitro release study

To study the behavior of the developed hydrogels as drug delivery systems, betamethasone as a model drug was loaded into them. The dry hydrogels (pieces of 40-70 mg) were immersed in 10 mL of 1mg/mL betamethasone solution for 24h. After incubation, the BTM-loaded hydrogels were taken out, rinsed with distiller water to remove the excess drug on the surface and dried at room temperature for 3 days. The loaded hydrogels were characterized by FTIR spectroscopy in order to know if they suffer any changed in the structure after incubation in BTM solution or if any chemical interaction between the drug and matrix occur

The amount of BTM loaded onto the hydrogels was estimated from the difference between the initial amount of drug in the solution and the amount remaining after absorption, determined spectrophotometrically at 242 nm using a BTM standard calibration curve.

$$BTM_{loaded} = C_1V_1 - C_2V_2 \qquad (3)$$

Where C_1 is the initial concentration of the loading BTM solution (mg/mL), V_1 is the initial volume of BTM solution (mL), C_2 and V_2 are the final concentration and remained volume of the BTM solution after the hydrogel's incubation.

The *in vitro* release studies were performed in PBS at pH 7.4, and 37°C. Briefly, the loaded hydrogels samples were incubated in 5 mL of PBS and at selected time intervals 0.5 mL of medium was extracted and replaced with equal volume of fresh PBS. The BTM concentration released was obtained by the same method mentioned above and the cumulative released amount (% BTM released) in each time was calculated, according to Equation 4.

$$\%BTM_{released} = \frac{m_r}{m_t} * 100 \qquad (4)$$

Where m_r is the released amount of BTM at selected time intervals and m_t is initial amount of BTM loaded in the dry hydrogels. Experiments were run in triplicate.

The release mechanism from AlgNa-g-poly(QCL-co-HEMA) hydrogels was investigated using release experimental data and the Korsmeyer-Peppas power law expression equation (Equation 2). [12]. In this case w_t is the mass released at time t and w_∞ is the total mass of BTM encapsulated in the matrix

3.5. Cell culture and cytotoxicity assay

Preprints (www.preprints.org) | NOT PEER-REVIEWED | Posted: 6 April 2021 doi:10.20944/preprints202104.0047.v2

Human chondrocyte C-28 and fibroblast 3T3 cells were cultured in Dulbecco´s modified Eagle´s medium (DMEM) containing 10% fetal bovine serum (FBS) and 1% antibiotics (penicillin-streptomycin) at 37°C under a 5% CO_2 humidified atmosphere.

The *in vitro* cytotoxicity of the hydrogels was evaluated based on their impact on cell structures like mitochondria by MTS assay (3-(4,5-dimethylthiazol-2-yl)-5-(3-carboxymethoxyphenyl)-2-(4-sulfophenyl)-2H-tetrazolium). The indirect extraction method to evaluated hydrogels samples cytotoxicity was used according to ISO 10993-5 standard and previous literature [21, 41]. The hydrogels extract solutions were prepared by incubating samples previously sterilized, in DMEM culture medium for 48 h at 37°C. After incubation, the extract solutions were filtered through a 0.22 μm syringe filter. Alternatively, C-28 and 3T3 cells were seeded in 96-well plates at a density of 1×10^4 cells per well and cultured in 5% CO_2 at 37°C for 24 h. Afterward, the medium in each well was replaced with 100 μL of the hydrogels extract solutions and the treated cells were incubated for 24, 48 and 72 h. After incubation time, the medium was discarded, the MTS solution was added and plates were incubated for another 3h in darkness. The absorbance of each well was measured by a micro-plate reader (VersaMax, Pennsylvania, USA; Program Softmax Pro) at 490 nm. Cells incubated only with DMEM culture medium were used as a negative control (100%), and the relative cell viability of the treated groups was calculated according to next equation.

$$\%\ Cell\ viability = \frac{OD_{samples}}{OD_{control}} \times 100 \qquad (5)$$

In order to evaluate de biocompatibility of materials after 7 days in contact with C28 and 3T3 cells the LIVE/DEAD assay were made. Live/dead is a quick and easy two-color assay where Calcein AM fluoresces green upon the reaction of intracellular esterase and stains live cells; ethidium homodimer-1, which binds to the DNA of dead membrane compromised cells, stains dead cells (red). First, small 2-3 mm thin disks of hydrogels were placed in 48 well plates overnight in DMEM medium. Then, the medium was removed, an aliquot of C28 human chondrocytes or C3T3 fibroblast suspension ($2x10^5$ cells), was seeded on the surface of the hydrogel disk and incubated for 6h at 5% CO_2 and 37°C to allow cell attachment. Subsequently, cell-seeded hydrogels were transferred into new 24-well plates, 1 mL of DMEM media was added on each well and incubated for 7 days. After every 24h, culture medium was replaced. At 7 days the hydrogels were rinsed with PBS and stained with Calcein AM/ethidium homodimer-1 using the Live-dead assay Kit (Invitrogen), according to the manufacturers' instructions. The images of the C28 and 3T3 cells on the surface hydrogels were captured by a fluorescence microscope (Leica DM 5500 B, Germany)

3.7 Statistical analysis

Graphs and statistics were performed with OriginPro 2018 (OriginLab Corp., Northampton, Massachusetts, USA). Data are reported as mean ± standard deviation (SD), unless stated otherwise. Error bars represent the SD calculated from tests of triplicate measurements for each scaffold. Statistical analysis was significant by a one-way analysis of variance (one-way ANOVA) for $p < 0.05$.

4. Conclusions

In this study a series of AlgNa-g-poly(QCL-co-HEMA) hydrogels were successfully synthesized by graft co-polymerization of QCL and HEMA onto the sodium alginate chain. Through FTIR characterization, it was possible to confirm the formation of graft co-polymer and the structural composition of these materials, constituted mainly by groups such as -OH, -COOH, -C=O and $N^+(CH_3)_3$. Morphological study shows that internal structure is porous in all samples. The hydrophilicity of the hydrogels was dependent upon the composition and pH medium, and the results of the kinetics study demonstrate that the swelling is conditioned by anomalous process. *In vitro* release of BTM loaded into the hydrogels were carried out during 8 h and the studies showed the effective way of BTM

release from hydrogels in controlled manner. In the case of *in vitro* cytocompatibility studies, it was confirmed through MTS and live/dead assays that samples from H1 to H5 are citocompatibles and allow the adhesion and cell proliferation against C28 and 3T3 cells, while in the sample H6 the cell viability was less than 20%. We can conclude that, AlgNa-g-poly(QCL-co-HEMA) hydrogels matrices obtained (compositions from H1 to H5) are promising materials for cartilage tissue engineering and drug delivery.

Author Contributions: J.G.-C., M.V., L.A., G.F., A.A., and L.J.C., conceptualization and methodology. J.G.-C., M.V., N.B., and L.A., investigation and data curation. G.F., A.A., J.A.-B., and O.V., investigation and formal analysis. J.G.-C., M.V., G.F., and O.V., writing—original draft preparation. J.G.-C., G.F., L.J.C., J.A.-B., and Y.T., writing—review and editing. L.J.C., J.A.-B., and Y.T., resources, supervision, project administration, and funding acquisition. All authors have read and agreed to the published version of the manuscript

Funding:

We would like to acknowledge the financial support from the European Union through Erasmus PLUS doctoral fellowship and mobility staff, project code 2015-1-NL01-KA 107-008639 (J. García, A. Almirall and G. Fuentes respctively). We also This work was also supported by project grants from the European Commission H2020-MSCA-RISE (644373—PRISAR), H2020-MSCA-RISE (777682—CANCER), H2020-WIDESPREAD-05-2017-Twinning (807281—ACORN), H2020-WIDESPREAD-2018-03 (852985—SIMICA), H2020-SCARISE-2016 (734684—CHARMED) and MSCA-ITN-2015-ETN (675743—ISPIC), 861190 (PAVE), 857894 (CAST), 859908 (NOVA-MRI); 872860 (PRISAR2). This work was also financially supported by the VIDI personal grant (project number 723.012.110) (Luis J. Cruz).

Institutional Review Board Statement: Not applicable

Informed Consent Statement: Not applicable

Data Availability Statement: Not applicable

Acknowledgments: Not applicable

Conflicts of Interest: The authors declare no conflict of interest

References

1. Kou, L., Xiao, S., Sun, R., Bao, S., Yao, Q. and Chen, R. Biomaterial-engineered intra-articular drug delivery systems for osteoarthritis therapy. *Drug Delivery* **2019**. *26*(*1*), 870-885.
2. Samuel, S., Ahmad, R.E., Ramasamy, T.S., Karunanithi, P., Naveen, S.V. and Kamarul, T. Platelet-rich concentrate in serum-free medium enhances cartilage-specific extracellular matrix synthesis and reduces chondrocyte hypertrophy of human mesenchymal stromal cells encapsulated in alginate. *Platelets* **2019**. *30*(*1*), 66-74.
3. Kaviani, A., Zebarjad, S.M., Javadpour, S., Ayatollahi, M. and Bazargan-Lari, R. Fabrication and characterization of low-cost freeze-gelated chitosan/collagen/hydroxyapatite hydrogel nanocomposite scaffold. *International Journal of Polymer Analysis and Characterization* **2019**. *24*(*3*), 191-203.
4. Silva, C.R., Babo, P.S., Gulino, M., Costa, L., Oliveira, J.M., Silva-Correia, J., Domingues, R.M.A., Reis, R.L. and Gomes, M.E. Injectable and tunable hyaluronic acid hydrogels releasing chemotactic and angiogenic growth factors for endodontic regeneration. *Acta Biomaterialia* **2018**. *77*155-171.
5. Urbanek, O., Kołbuk, D. and Wróbel, M. Articular cartilage: New directions and barriers of scaffolds development – review. *International Journal of Polymeric Materials and Polymeric Biomaterials* **2019**. *68*(*7*), 396-410.
6. Wang, J., Wang, Y., Sun, X., Liu, D., Huang, C., Wu, J., Yang, C. and Zhang, Q. Biomimetic cartilage scaffold with orientated porous structure of two factors for cartilage repair of knee osteoarthritis. *Artificial Cells, Nanomedicine, and Biotechnology* **2019**. *47*(*1*), 1710-1721.

7. Passos, M.F., Carvalho, N.M.S., Rodrigues, A.A., Bavaresco, V.P., Jardini, A.L., Maciel, M.R.W. and Maciel Filho, R. PHEMA Hydrogels Obtained by Infrared Radiation for Cartilage Tissue Engineering. *International Journal of Chemical Engineering* **2019**. *20194*249581.
8. Khalid, I., Ahmad, M., Minhas, M.U. and Barkat, K. Preparation and characterization of alginate-PVA-based semi-IPN: controlled release pH-responsive composites. *Polymer Bulletin* **2018**. *75*(*3*), 1075-1099.
9. Torres, M.L., Oberti, T.G. and Fernández, J.M. HEMA and alginate-based chondrogenic semi-interpenetrated hydrogels: synthesis and biological characterization. *Journal of Biomaterials Science, Polymer Edition* **2020**. 1-20.
10. Hasnain, M.S., Ray, P. and Nayak, A.K. Chapter 5 - Alginate-based interpenetrating polymer networks for sustained drug release. In *Alginates in Drug Delivery*, A.K. Nayak and M.S. Hasnain, Editors., Academic Press. 2020101-128.
11. Farokhi, M., Jonidi Shariatzadeh, F., Solouk, A. and Mirzadeh, H. Alginate Based Scaffolds for Cartilage Tissue Engineering: A Review. *International Journal of Polymeric Materials and Polymeric Biomaterials* **2020**. *69*(*4*), 230-247.
12. Goel, N.K., Kumar, V., Bhardwaj, Y.K., Chaudhari, C.V., Dubey, K.A. and Sabharwal, S. Swelling Response of Radiation Synthesized 2-Hydroxyethylmethacrylate-co-[2-(methacryloyloxy)ethyl] Trimethylammonium Chloride Hydrogels Under Various In Vitro Conditions. *Journal of Biomaterials Science, Polymer Edition* **2009**. *20*(*5-6*), 785-805.
13. Bölgen, N., Yang, Y., Korkusuz, P., Güzel, E., El Haj, A.J. and Pişkin, E. 3D ingrowth of bovine articular chondrocytes in biodegradable cryogel scaffolds for cartilage tissue engineering. *J Tissue Eng Regen Med* **2011**. *5*(*10*), 770-9.
14. Nicolas, C., Verny, M., Giraud, I., Ollier, M., Rapp, M., Maurizis, J.-C. and Madelmont, J.-C. New Quaternary Ammonium Oxicam Derivatives Targeted toward Cartilage: Synthesis, Pharmacokinetic Studies, and Antiinflammatory Potency. *Journal of Medicinal Chemistry* **1999**. *42*(*25*), 5235-5240.
15. Rivero, R., Alustiza, F., Capella, V., Liaudat, C., Rodriguez, N., Bosch, P., Barbero, C. and Rivarola, C. Physicochemical properties of ionic and non-ionic biocompatible hydrogels in water and cell culture conditions: Relation with type of morphologies of bovine fetal fibroblasts in contact with the surfaces. *Colloids and Surfaces B: Biointerfaces* **2017**. *158*488-497.
16. Giraud, I., Rapp, M., Maurizis, J.-C. and Madelmont, J.-C. Application to a Cartilage Targeting Strategy: Synthesis and in Vivo Biodistribution of 14C-Labeled Quaternary Ammonium−Glucosamine Conjugates. *Bioconjugate Chemistry* **2000**. *11*(*2*), 212-218.
17. Miot-Noirault, E., Vidal, A., Morlieras, J., Bonazza, P., Auzeloux, P., Besse, S., Dauplat, M.-M., Peyrode, C., Degoul, F., Billotey, C., Lux, F., Rédini, F., Tillement, O., Chezal, J.-M., Kryza, D., and Janier, M. Small rigid platforms functionalization with quaternary ammonium: Targeting extracellular matrix of chondrosarcoma. *Nanomedicine: Nanotechnology, Biology and Medicine* **2014**. *10*(*8*), 1887-1895.
18. Zhu, Z. and Zhu, Z. Adhesion of starch-g-poly(2-acryloyloxyethyl trimethyl ammonium chloride) to cotton and polyester fibers. *Starch - Stärke* **2014**. *66*(*5-6*), 566-575.
19. Shen, S., Zhu, Z. and Liu, F. Introduction of poly[(2-acryloyloxyethyl trimethyl ammonium chloride)-co-(acrylic acid)] branches onto starch for cotton warp sizing. *Carbohydrate Polymers* **2016**. *138*280-289.
20. Bardajee, G.R., Hooshyar, Z. and Rastgo, F. Kappa carrageenan-g-poly (acrylic acid)/SPION nanocomposite as a novel stimuli-sensitive drug delivery system. *Colloid and Polymer Science* **2013**. *291*(*12*), 2791-2803.
21. Hu, X., Wang, Y., Zhang, L., Xu, M., Dong, W. and Zhang, J. Redox/pH dual stimuli-responsive degradable Salecan-g-SS-poly(IA-co-HEMA) hydrogel for release of doxorubicin. *Carbohydrate Polymers* **2017**. *155*242-251.
22. Natchimuthu, I.C.a.N. Hydrogels of sodium alginate based copolymers grafted with sodium-2-acrylamido-2-methyl-1-propane sulfonate and methacrylic acid for controlled drug delivery applications. *Journal of Macromolecular Science, Part A* **2018**. *55*(*2*), 168-175.
23. Mandal, B. and Ray, S.K. Synthesis of interpenetrating network hydrogel from poly(acrylic acid-co-hydroxyethyl methacrylate) and sodium alginate: Modeling and kinetics study for removal of synthetic dyes from water. *Carbohydrate Polymers* **2013**. *98*(*1*), 257-269.

24. Jiang, H., Yang, Y., Lin, Z., Zhao, B., Wang, J., Xie, J. and Zhang, A. Preparation of a novel bio-adsorbent of sodium alginate grafted polyacrylamide/graphene oxide hydrogel for the adsorption of heavy metal ion. *Science of The Total Environment* **2020**. *744*140653.
25. Rivas, B.L. and Aguirre, M.D.C. Water-soluble polymers: Optimization of arsenate species retention by ultrafiltration. *Journal of Applied Polymer Science* **2009**. *112*(*4*), 2327-2333.
26. Torres, C.C., Urbano, B.F., Campos, C.H., Rivas, B.L. and Reyes, P. Composite hydrogel based on surface modified mesoporous silica and poly[(2-acryloyloxy)ethyl trimethylammonium chloride]. *Materials Chemistry and Physics* **2015**. *15*269-76.
27. Lee, B.-S., Chen, Y.-J., Wei, T.-C., Ma, T.-L. and Chang, C.-C. Comparison of Antibacterial Adhesion When Salivary Pellicle Is Coated on Both Poly(2-hydroxyethyl-methacrylate)- and Polyethylene-glycol-methacrylate-grafted Poly(methyl methacrylate). *International Journal of Molecular Sciences* **2018**. *19*(*9*), 2764.
28. Zhang, L., Zheng, G.-J., Guo, Y.-T., Zhou, L., Du, J. and He, H. Preparation of novel biodegradable pHEMA hydrogel for a tissue engineering scaffold by microwave-assisted polymerization. *Asian Pacific Journal of Tropical Medicine* **2014**. *7*(*2*), 136-140.
29. Yang, X., Wang, B., Qiao, C., Li, Z., Li, Y., Xu, C. and Li, T. Molecular interactions in N-[(2-hydroxyl)-propyl-3-trimethyl ammonium] chitosan chloride-sodium alginate polyelectrolyte complexes. *Food Hydrocolloids* **2020**. *100*105400.
30. Onder, A., Ilgin, P., Ozay, H. and Ozay, O. Removal of dye from aqueous medium with pH-sensitive poly[(2-(acryloyloxy)ethyl]trimethylammonium chloride-co-1-vinyl-2-pyrrolidone] cationic hydrogel. *Journal of Environmental Chemical Engineering* **2020**. *8*(*5*), 104436.
31. Vargün, E. and Usanmaz, A. Degradation of Poly(2-hydroxyethyl methacrylate) Obtained by Radiation in Aqueous Solution. *Journal of Macromolecular Science, Part A* **2010**. *47*(*9*), 882-891.
32. El-Sherbiny, I.M., Abdel-Mogib, M., Dawidar, A.-A.M., Elsayed, A. and Smyth, H.D.C. Biodegradable pH-responsive alginate-poly (lactic-co-glycolic acid) nano/micro hydrogel matrices for oral delivery of silymarin. *Carbohydrate Polymers* **2011**. *83*(*3*), 1345-1354.
33. Das, D., Pham, H.T.T., Lee, S. and Noh, I. Fabrication of alginate-based stimuli-responsive, non-cytotoxic, terpolymric semi-IPN hydrogel as a carrier for controlled release of bovine albumin serum and 5-amino salicylic acid. *Materials Science & Engineering C* **2019**. *98*42-53.
34. Ghobashy, M.M. and Bassioni, G. pH stimuli-responsive poly(acrylamide-co-sodium alginate) hydrogels prepared by γ-radiation for improved compressive strength of concrete. *Advances in Polymer Technology* **2018**. *37*(*6*), 2123-2133.
35. Dou, W.-h., Zhou, G.-m. and Kang, Q.-q. Study of the Epimers of Dexamethasone Sodium Phosphate and Betamethasone Sodium Phosphate by FTIR, FT-Raman and SERS. *Spectroscopy and Spectral Analysis* **2012**. *32*(*10*), 2664-2668.
36. Monajjemzadeh, F., Gholizadeh, N., Yousefzadeh Mobaraki, N. and Jelvehgari, M. Physicochemical and in vitro mucoadhesive properties of microparticles/discs of betamethasone for the management of oral lichen planus. *Pharmaceutical Development and Technology* **2016**. *21*(*8*), 996-1005.
37. Ghasemnejad, M., Ahmadi, E., Mohamadnia, Z., Doustgani, A. and Hashemikia, S. Functionalized silica nanoparticles as a carrier for Betamethasone Sodium Phosphate: Drug release study and statistical optimization of drug loading by response surface method. *Materials Science and Engineering: C* **2015**. *56*223-232.
38. Dalapati, S., Alam, M.A., Jana, S. and Guchhait, N. Reduced Schiff-base assisted novel dihydrogenphosphate–water polymer. *CrystEngComm* **2012**. *14*(*18*), 6029-6034.
39. Basaran, I., Emami Khansari, M., Pramanik, A., Wong, B.M. and Hossain, M.A. Binding and selectivity of dihydrogen phosphate by H-bond donors and acceptors in a tripodal-based thiourea receptor. *Tetrahedron Letters* **2015**. *56*(*1*), 115-118.
40. Kim, A.R., Lee, S.L. and Park, S.N. Properties and in vitro drug release of pH- and temperature-sensitive double cross-linked interpenetrating polymer network hydrogels based on hyaluronic acid/poly (N-isopropylacrylamide) for transdermal delivery of luteolin. *International Journal of Biological Macromolecules* **2018**. *118*731-740.

 doi:10.20944/preprints202104.0047.v2

41. Roointan, A., Farzanfar, J., Mohammadi-Samani, S., Behzad-Behbahani, A. and Farjadian, F. Smart pH responsive drug delivery system based on poly(HEMA-co-DMAEMA) nanohydrogel. *International Journal of Pharmaceutics* **2018**. *552*(*1*), 301-311.